



Effects of injection conditions on the stability of rotating detonation waves

S. Zhang¹ · S. Yao¹ · M. Luan¹ · L. Zhang¹ · J. Wang¹ 

Received: 31 October 2017 / Revised: 29 June 2018 / Accepted: 9 July 2018 / Published online: 27 July 2018
© Springer-Verlag GmbH Germany, part of Springer Nature 2018

Abstract

This article presents a numerical investigation of a rotating detonation engine (RDE). The simulation explores the instability mechanism of detonation waves in the RDE with micro-convergent-nozzle injection. The process is modeled by the two-dimensional reactive Euler equations with detailed chemical reaction kinetics for the injection of premixed stoichiometric hydrogen–air. The numerical results show an interesting instability phenomenon whereby an unstable detonation wave rotates circumferentially at the fuel injection head of the chamber. The shape of the fresh fuel layer is irregular, which is different from that in previous numerical simulations. The height and strength of the detonation wave are periodically fluctuating, as well as the mass flow rate of the reactants into the chamber. Based on the time evolution of the detonation wave, it is found that the detonation wave oscillates due to the interaction of fuel injection and weak transverse shock waves following the detonation wave. The detonation wave, the shape of the fresh fuel layer, and the mass flow rate influence each other. Therefore, this oscillation remains in the flow field, as does the instability of the detonation wave. This finding is in good agreement with previous experiments.

Keywords Rotating detonation · Instability · Micro-convergent nozzles · Detonation engine

1 Introduction

Detonation is a supersonic combustion phenomenon characterized by the coupling of a shock wave with the chemical reaction heat release behind it. Compared with conventional combustion, detonation allows more intense, more thermodynamically beneficial, and more stable burning of various fuels in smaller chambers. Because of these advantages, detonation waves have been explored extensively for propulsion applications. Among all engines based on detonation combustion, the rotating detonation engine (RDE) has received increasing attention worldwide due to its inherently higher thermodynamic efficiency and excellent propulsion performance, compared with conventional rocket engines and turbojet engines that

are based on constant-pressure combustion. The RDE has great potential to become a supersonic propulsion system.

The basic concept of rotating detonation waves was proposed by Voitsekhovskii [1] in the 1960s. He experimentally achieved a short-lived rotating detonation wave in a disk-shaped chamber, using premixed acetylene and oxygen. In the following 20 years, little attention was paid to the development of the RDE. In the mid-1990s, extensive testing of the RDE was resumed in the Institute of Hydrodynamics by Bykovskii et al. [2]. They carried out a series of experimental research programs on the RDE, in various geometries using different fuels. They made remarkable achievements in verifying the feasibility of the RDE. Then, mainly due to the promotion of Wolanski [3, 4], the RDE has become a focus of research worldwide. Currently, there are many research groups working on the RDE in Russia [5, 6], USA [7–9], Japan [10, 11], France [12, 13], and China [14–16]. Advancements have been obtained not only in numerical simulations but also in experiments.

For propulsion systems, it is an essential requirement for the RDE to run stably. However, under practical condi-

Communicated by G. Ciccarelli.

✉ J. Wang
wangjp@pku.edu.cn

¹ Center for Combustion and Propulsion, CAPT and SKLTCS, Department of Mechanics and Engineering Science, College of Engineering, Peking University, Beijing 100871, People's Republic of China

tions, detonation waves are not always stable. The detonation propagation mode depends on the engine design parameters, including the chamber geometry, injection conditions, and the mass flow rate of reactants. Previous experiments have shown that when the engine design parameters are changed, unstable detonation propagation processes can be observed. Some researchers paid attention to the effect of the mass flow rate on the stability of the RDE. Bykovskii et al. [17] found that higher mass flow rates generally result in more detonation waves in the RDE. Wolanski [3] pointed out that it was necessary to create a sufficient volume of fresh mixture ahead of the detonation waves for the stable operation of the RDE. They proposed a new parameter, the so-called detonation wave number, to judge whether the detonation waves are stable or not. The experimental results obtained by Liu et al. [18] showed that the strength of detonation waves oscillated periodically when the mass flow rate increased. Wu et al. [19] numerically simulated this phenomenon by increasing the injection total pressure to increase the mass flow rate into the RDE. Other researchers analyzed the instability phenomenon in the RDE. According to the fluctuation frequency of the experimental pressure history, Wang et al. [20] found that these instability phenomena fall into three categories: low-frequency, intermediate-frequency, and high-frequency detonation instabilities. Anand et al. [21] found a similar low-frequency instability phenomenon in experiments. They both determined that the low-frequency instability was caused by the interaction of the fuel injection and the detonation waves. Subsequently, Anand et al. [9] identified four kinds of fundamental instabilities in the RDE. They proposed that this low-frequency instability may be due to a low-frequency oscillation in the air inlet, which in turn may be generated by Helmholtz resonance instigated in the air inlet by the rotating detonation wave. Nevertheless, due to the difficulty of three-dimensional visualization of the RDE flow field, it is difficult to explain the mechanism behind this low-frequency instability.

In this study, a two-dimensional numerical simulation is performed to further explore the mechanism of this low-frequency instability. The injection velocity and pressure at the inlet wall are discussed based on the time evolution of detonation waves. The pressure gradient in the overall flow field is evaluated to reveal the interaction between the injection of fresh gas and the detonation wave.

2 Physical modeling and numerical method

2.1 Physical modeling

The RDE chamber is a coaxial annular cavity. Detonation waves propagate azimuthally in the annulus, while com-

bustible mixture is injected from the head end, and the burnt gas leaves out of the downstream exit. The width of the annulus is much smaller than the outer radius, and therefore, a “zero” thickness can be assumed, as shown in Fig. 1a. Figure 1b shows the numerical simulation field by unraveling the thin chamber to a plane. In the present study, the radius and length of the RDE are 0.01 and 0.05 m, respectively.

The premixed stoichiometric hydrogen–air mixture is injected into the chamber through a large number of micro-convergent nozzles distributed uniformly on the injection wall (edge 2 in Fig. 1b). The injection stagnation pressure p_0 and temperature T_0 are set to 0.5 MPa and 360 K, respectively. From the isentropic relationship, the corresponding critical pressure p_{cr} is 0.264 MPa. The injection boundary condition is specified according to the local pressure p_w just near the wall. (1) When $p_w \geq p_0$, the reaction mixture is not injected into the chamber, i.e., rigid wall condition is set locally. (2) When $p_{cr} < p_w < p_0$, the injection condition is evaluated from the isentropic relationship and the injection is subsonic. (3) When $p_w \leq p_{cr}$, the injection is not affected by the wall pressure and the injection is sonic. At the exit (edge 3 in Fig. 1b), the type of boundary condition depends on the local flow state. (1) The exit pressure sets the ambient pressure $p_\infty = 0.1$ MPa when the exhaust gas speed is subsonic. (2) When the exhaust gas speed is supersonic, the exit pressure is extrapolated from the values in the chamber. The edges 1a and 1b are set to periodic boundary conditions. The boundary conditions are similar to those used in [10, 22].

A section of a typical one-dimensional detonation wave is placed at the head-end region I to initiate the two-dimensional detonation, as shown in Fig. 1. Region II is initially filled with premixed stoichiometric hydrogen–air mixtures at a pressure of 0.1 MPa and temperature of 300 K.

2.2 Numerical method

The flow field is governed by the two-dimensional (cylindrical coordinates are used) conservative reactive Euler equations. Viscosity, thermal conduction, and mass diffusion are ignored in this study, similar to [10, 11, 14, 15, 22]. Euler equations with source terms in cylindrical coordinates are expressed as:

$$\frac{\partial U}{\partial t} + \frac{\partial F}{\partial \theta} + \frac{\partial G}{\partial z} = S, \quad (1)$$

where the conservative variable vector U , the convective flux vectors F and G , and the source vector S are, respectively, defined as:

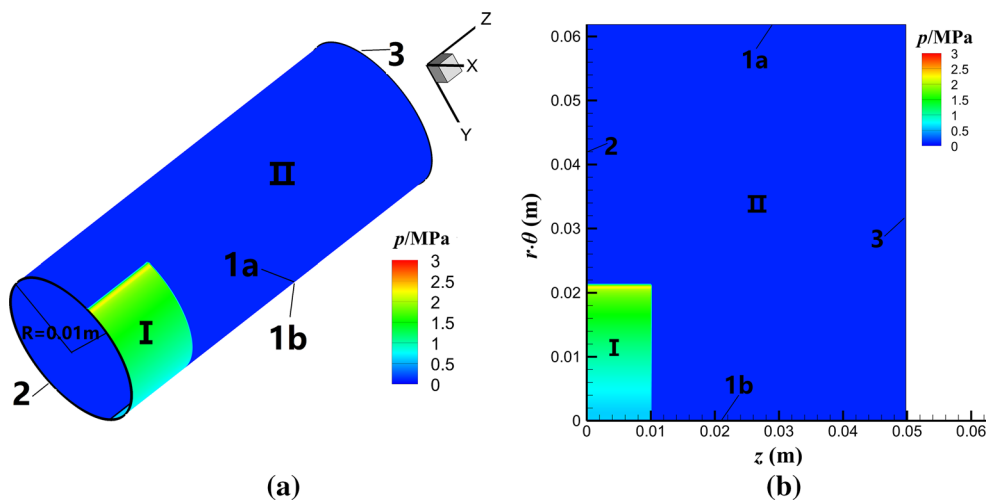


Fig. 1 Physical model. **a** Schematic of the RDE. **b** Two-dimensional plane model

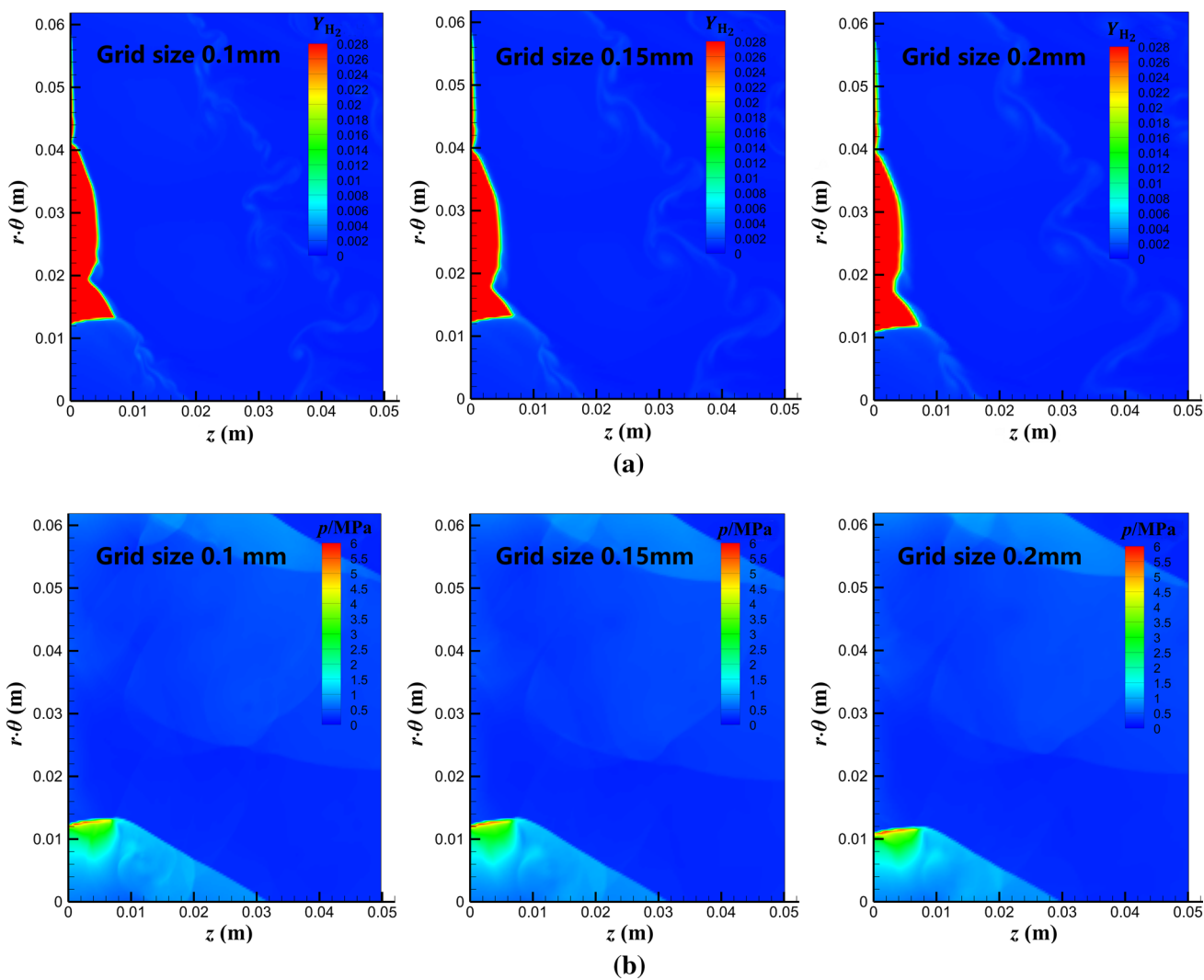


Fig. 2 Comparison of the detonation flow field for three grid sizes. **a** Contours of the hydrogen mass fraction for three grid sizes. **b** Pressure contours for three grid sizes

$$U = \begin{bmatrix} \rho \\ \rho u_\theta \\ \rho u_z \\ E \\ \rho_i \end{bmatrix} \quad F = \frac{1}{r} \begin{bmatrix} \rho u_\theta \\ \rho u_\theta^2 + p \\ \rho u_z u_\theta \\ u_\theta(E + p) \\ \rho_i u_\theta \end{bmatrix}$$

$$G = \begin{bmatrix} \rho u_z \\ \rho u_\theta u_z \\ \rho u_z^2 + p \\ u_z(E + p) \\ \rho_i u_z \end{bmatrix} \quad S = \begin{bmatrix} 0 \\ 0 \\ 0 \\ 0 \\ \dot{\omega}_i \end{bmatrix}. \quad (2)$$

The total energy per unit volume E is defined as:

$$E = \sum \rho_i h_i - p + \frac{1}{2} \rho (u_\theta^2 + u_z^2), \quad (3)$$

where h_i is the specific enthalpy of the i th species (J/kg). The density of the i th species is expressed as:

$$\rho_i = \rho Y_i, \quad (4)$$

where Y_i is the mass fraction of the i th species. The production rate $\dot{\omega}_i$ of the i th species is obtained using detailed chemical reaction kinetics for hydrogen–air [23]. The thermodynamic properties are approximated by polynomial

expressions as a function of the temperature. The coefficients of the polynomials are obtained from the JANAF tables [24].

The Strang's operator splitting method is employed to split the fluid flow and the chemical reaction. The convective flux terms are solved by the fifth-order monotonicity-preserving weighted essentially non-oscillatory scheme (MPWENO), and the time integration is performed by a third-order total variation diminishing (TVD) Runge–Kutta method. The chemical reaction source terms are treated in a linearly point-implicit manner to avoid the stiffness problem.

3 Results and discussion

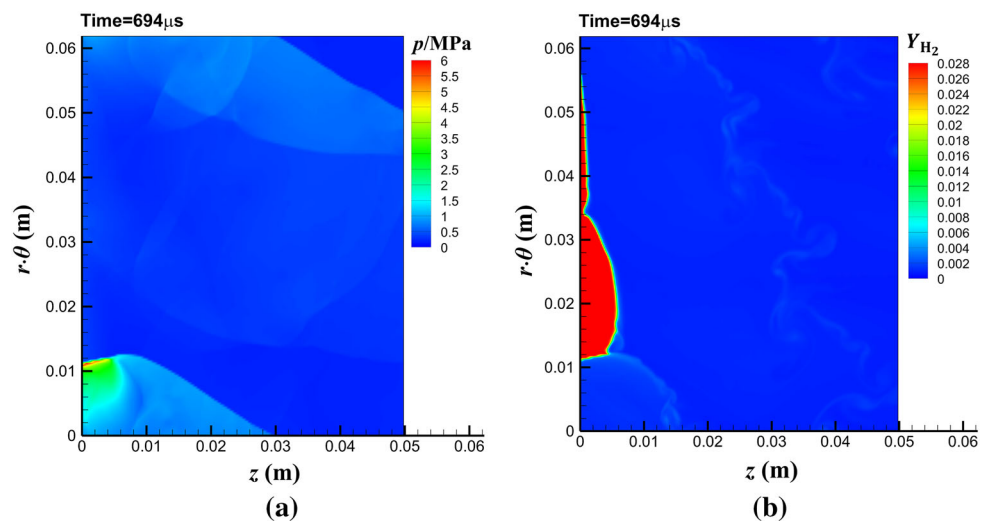
3.1 Grid dependency

The detonation flow field for a premixed stoichiometric hydrogen–air mixture for three computational grid sizes of 0.1, 0.15, and 0.2 mm is shown in Fig. 2. It is found that the three grid sizes produce the same detonation flow field, especially the irregular shape of the fresh fuel layer shown in Fig. 2a. To further validate the grid dependency, comparison of detonation wave height and velocity for the three grid sizes is given in Table 1. It can be seen that the detonation wave heights are similar, as well as the detonation velocities, although the detonation velocity with grid size of 0.1 mm is slightly larger than those with grid sizes of 0.15 and 0.2 mm. Furthermore, the detonation velocities are all over 96% of the theoretical CJ detonation velocity of 2000.3 m/s, which validates the numerical method. The aim of this study is to investigate the instability in the RDE, but not the micro-cells or detailed wave structures. Considering the computational cost, the grid size of 0.15 mm was used in the present study.

Table 1 Comparison of the detonation wave height and velocity for three grid sizes

Grid size (mm)	Detonation wave height (mm)	Detonation velocity (m/s)
0.1	6.7	1932.3
0.15	6.6	1926.4
0.2	6.6	1926.4

Fig. 3 Instantaneous contours at 694 μ s. **a** Pressure contour. **b** Contour of the hydrogen mass fraction



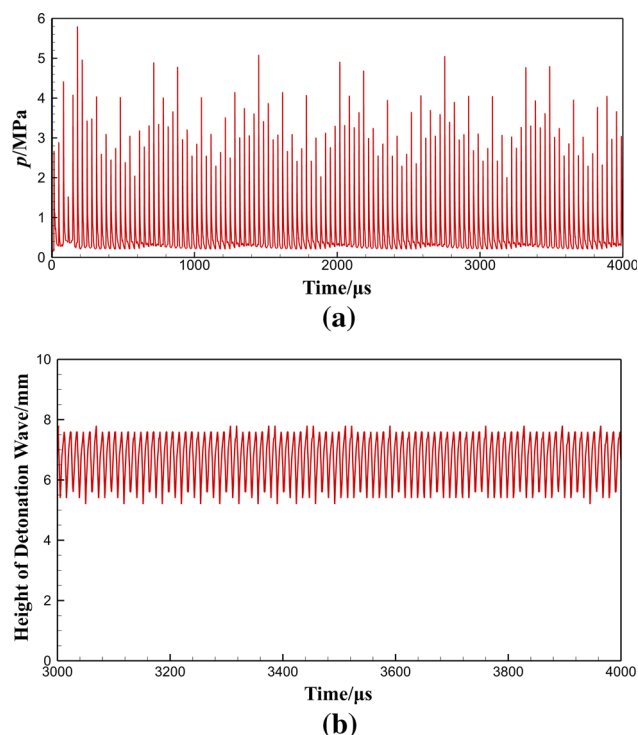


Fig. 4 Temporal evolution of pressure and detonation wave height. **a** Pressure history of detonation wave. **b** Temporal evolution of detonation wave height

3.2 Instability mechanism in the RDE

A detonation wave forms that rotates circumferentially at the head of the chamber, as shown in Fig. 3. Figure 4 shows the periodic oscillations of the height and strength of the detonation wave. A similar phenomenon has been seen in previous experiments [9, 20, 21]. The average cycle period and the detonation velocity are $32.5 \mu\text{s}$ and 1932.3 m/s , respectively. The velocity is 96.6% of the theoretical CJ value (about 2000.3 m/s) under the same conditions.

The fresh gas injection velocity with respect to time at points located between point A (0, 0.0121) and point C (0, 0.0554) is recorded, and their integral obtained by the Newton–Cotes formula is calculated from 670 to $694 \mu\text{s}$, forming the border line of the fresh fuel layer, as shown in Fig. 5. The border line of the fresh fuel layer given by the integral calculation is in good agreement with that obtained from the simulation, especially point B. Therefore, the irregular shape of the fresh fuel layer is caused by injection conditions. Nine points near the point B are evenly spaced between point (0, 0.032) and point (0, 0.038), where pressures and injection velocities at these points with respect to time are recorded, as shown in Fig. 6. The detonation pressure rises successively from point 1 to point 9. Afterward, the pressure at each point declines gradually due to the effect of rarefaction waves. The

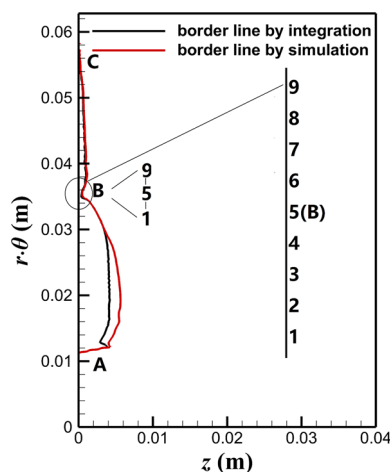


Fig. 5 Borderline of the fresh fuel layer

fresh fuel is injected into the chamber when p_0 is higher than the local chamber pressure at each point.

As shown in Fig. 6a, the fresh fuel is successively injected into the chamber through points 1, 2, and 3. The fuel injection is continuous at these three points, whose pressures are always lower than p_0 , though there are several slight pressure oscillations observed after the front passes. The pressure oscillations at points 4, 5, and 6 are so large that sometimes the pressure becomes greater than p_0 , as shown in Fig. 6b. As a result, the injection is cut off for a period of time until the pressure becomes lower than p_0 . The situation at points 7, 8, and 9 is similar to that at points 1, 2, and 3, as shown in Fig. 6c. The only difference is that the total time for injection at point 7, 8, and 9 is shorter.

The accumulation of fresh gas at each point is calculated from 670 to $694 \mu\text{s}$. The results are given in Table 2. Point 5 (overlapping with point B) has the smallest accumulation of fresh gas, which explains why the detonation height is minimum in Fig. 5.

Figure 7 shows that the pressure profile along the inlet wall varies with a fixed shape. Furthermore, the pressure in each location of the inlet wall is greater than p_{cr} . Therefore, the inlet micro-convergent nozzles are not choked. And pressure oscillations can affect the injection velocity at each nozzle. Because the height and strength of the detonation wave oscillate periodically, the pressure oscillation in the flow field must be periodic. As a consequence, the mass flow rate is periodically fluctuating, as shown in Fig. 8. The fluctuating mass flow rate can, in turn, aggravate oscillations in the flow field.

The calculated logarithmic pressure gradient contours are shown in Fig. 9. From 671.5 to $678.5 \mu\text{s}$, the height of the detonation wave changes from the lowest to the highest

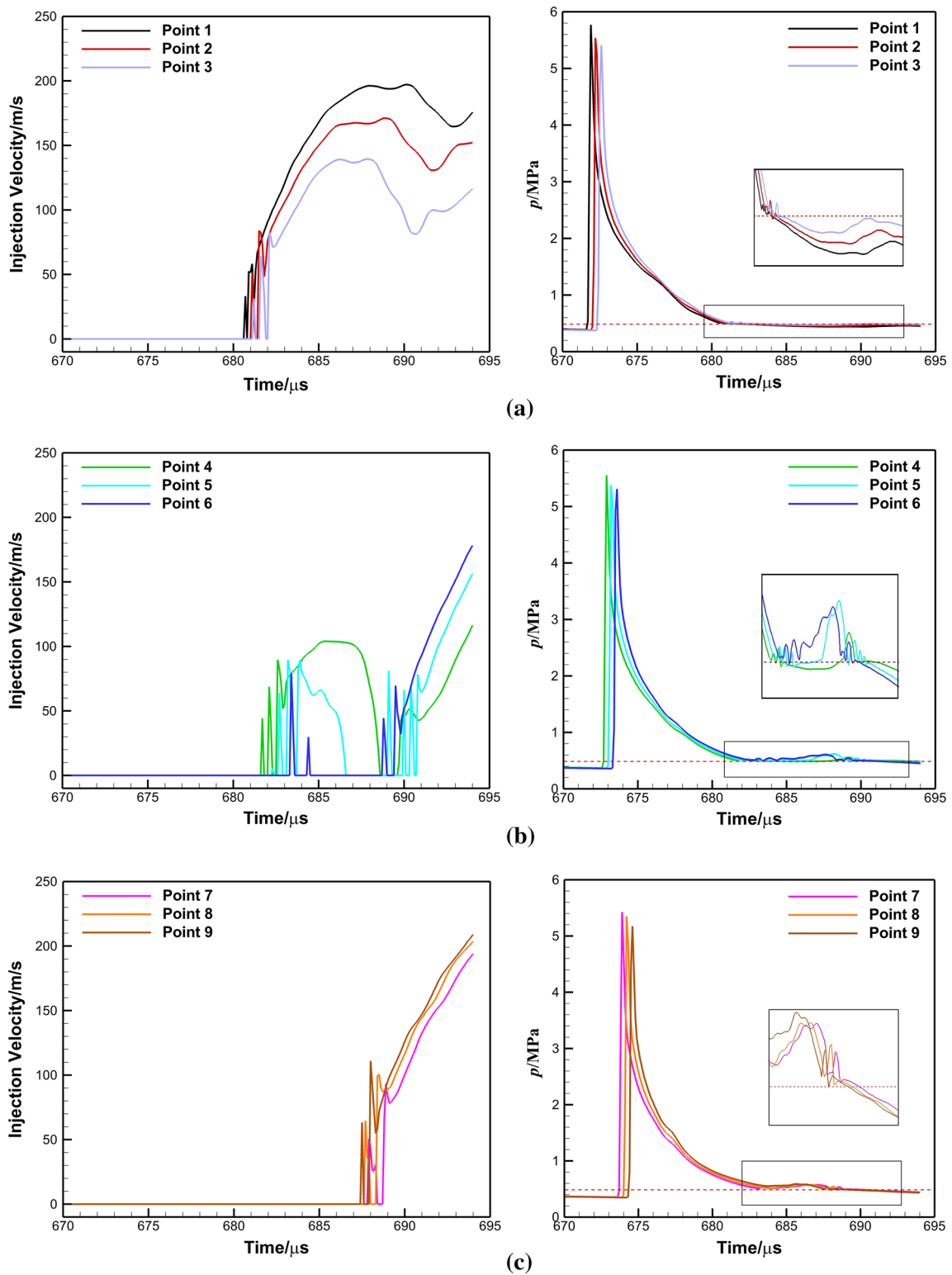


Fig. 6 Temporal evolution of the injection velocity and pressure at points 1–9. **a** Temporal evolution of injection velocities and pressures at points 1–3. **b** Temporal evolution of injection velocities and pressures at points 4–6. **c** Temporal evolution of injection velocities and pressures at points 7–9

Table 2 Accumulation of fresh gas at points 1–9

Points	Point 1	Point 2	Point 3	Point 4	Point 5	Point 6	Point 7	Point 8	Point 9
Accumulation of fresh gas (mm)	2.2	1.8	1.4	0.8	0.5	0.6	0.7	0.8	0.9

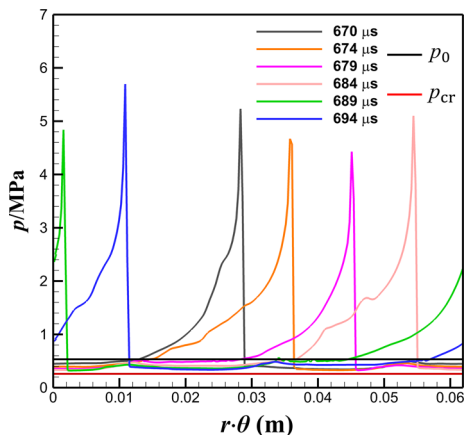


Fig. 7 Pressure distribution of overall inlet wall

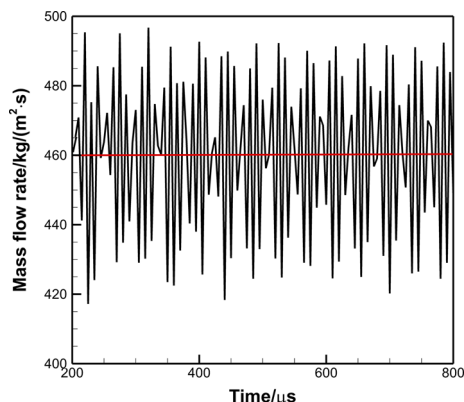


Fig. 8 Temporal evolution of mass flow rate

and then reaches the lowest again at 682.7 μs . The periodic oscillation of the detonation wave height produces a group of transverse weak shock waves, making the flow field extremely complicated. These weak shock waves propagate to the inlet wall, collide with it, reflect, and then spread

downstream. At 686.6 μs , some weak shock waves collide with the fresh fuel layer (at point B or point 5 in Fig. 5), producing a local pressure which is greater than p_0 . As a result, the fuel injection is cut off until to 690.8 μs . However, fresh gas starts to be injected through point 7, 8, and 9 (see Fig. 5), when point B (point 5) is blocked. The process coincides with the evolution of the velocity at point 5 in Fig. 6b. Weak shock waves also collide with the fresh fuel layer at points 1–4 and points 6–9, but the pressure oscillations caused by these waves are so slight as not to block fuel injection at these points. This coincides well with the phenomena in Fig. 6a, c.

4 Conclusions

A two-dimensional numerical simulation of the RDE with detailed chemical reaction kinetics for the premixed stoichiometric hydrogen–air mixture was carried out. The instability mechanism of detonation waves manifested as oscillations in the wave height and strength in the RDE with micro-convergent-nozzle injection was explored. The detonation wave oscillates due to the interaction between fuel injection and the detonation wave. The oscillation of the detonation wave produces a group of weak shock waves, making the flow field very complicated. Some weak shock waves collide with the inlet wall, producing an instant pressure rise greater than the injection stagnation pressure, which stops the fuel injection at these high-pressure locations. Simultaneously, fresh fuel can be injected into the chamber near the blocked locations. As a consequence, the fresh fuel layer height varies with time, which in turn causes the detonation wave to oscillate. Furthermore, the micro-convergent nozzles are not choked, and therefore, the mass flow rate fluctuates due to pressure oscillations. The fluctuating mass flow rate can aggravate oscillations in the flow field, contributing to the fresh fuel layer irregularity. This irregularity remains in the flow field, as does the instability of the detonation wave.

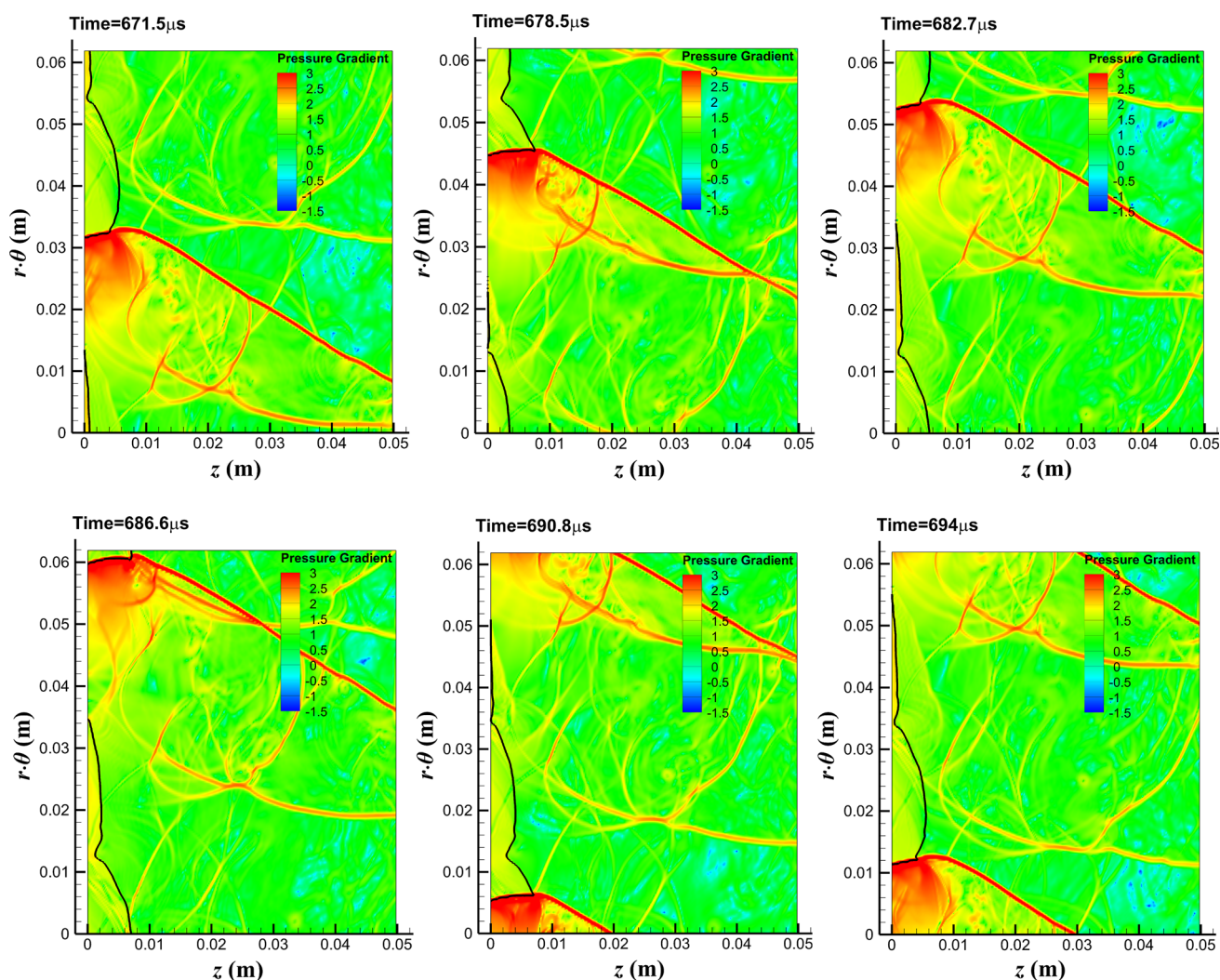


Fig. 9 Logarithmic pressure gradient contours at six times. The black line represents the borderline of the fresh fuel layer

Acknowledgements This research has been supported by the National Natural Science Foundation of China (Grant No. 91741202).

References

1. Voitsekhovskii, B.V.: Stationary spin detonation. *Dokl. Akad. Nauk SSSR* **129**, 1254–1256 (1959)
2. Bykovskii, F.A., Vedernikov, E.F.: Continuous detonation combustion of an annular gas-mixture layer. *Combust. Explos. Shock Waves* **32**, 489–491 (1996). <https://doi.org/10.1007/BF01998570>
3. Wolański, P.: Rotating detonation wave stability. In: 23rd International Colloquium on the Dynamics of Explosions and Reactive Systems, Paper 211, Irvine, CA, USA (2011)
4. Wolański, P.: Detonative propulsion. *Proc. Combust. Inst.* **34**, 125–158 (2013). <https://doi.org/10.1016/j.proci.2012.10.005>
5. Dubrovskii, A.V., Ivanov, V.S., Frolov, S.M.: Three-dimensional numerical simulation of the operation process in a continuous detonation combustor with separate feeding of hydrogen and air. *Russ. J. Phys. Chem. B* **9**, 104–119 (2015). <https://doi.org/10.1134/S190793115010157>
6. Frolov, S.M., Aksenov, V.S., Ivanov, V.S., Shamshin, I.O.: Large-scale hydrogen–air continuous detonation combustor. *Int. J. Hydrogen Energy* **40**, 1616–1623 (2015). <https://doi.org/10.1016/j.ijhydene.2014.11.112>
7. Fotia, M.L., Schauer, F., Kaemming, T., Hoke, J.: Experimental study of the performance of a rotating detonation engine with nozzle. *J. Propuls. Power* **32**, 674–681 (2016). <https://doi.org/10.2514/1.B35913>
8. Schwer, D., Kailasanath, K.: Fluid dynamics of rotating detonation engines with hydrogen and hydrocarbon fuels. *Proc. Combust. Inst.* **34**, 1991–1998 (2013). <https://doi.org/10.1016/j.proci.2012.05.046>
9. Anand, V., St. George, A., Driscoll, R., Gutmark, E.: Characterization of instabilities in a rotating detonation combustor. *Int. J. Hydrogen Energy* **40**, 16649–16659 (2015). <https://doi.org/10.1016/j.ijhydene.2015.09.046>
10. Tsuboi, N., Watanabe, Y., Kojima, T., Hayashi, A.K.: Numerical estimation of the thrust performance on a rotating detonation engine for a hydrogen–oxygen mixture. *Proc. Combust. Inst.* **35**, 2005–2013 (2015). <https://doi.org/10.1016/j.proci.2014.09.010>
11. Fujii, J., Kumazawa, Y., Matsuo, A., Nakagami, S., Matsuoka, K., Kasahara, J.: Numerical investigation on detonation velocity

- in rotating detonation engine chamber. *Proc. Combust. Inst.* **36**, 2665–2672 (2017). <https://doi.org/10.1016/j.proci.2016.06.155>
12. Le Naour, B., Falempin, F., Coulon, K.: MBDA R&T effort regarding continuous detonation wave engine for propulsion—Status in 2016. 21st AIAA International Space Planes and Hypersonics Technologies Conference, Xiamen, China, AIAA Paper 2017-2325 (2017). <https://doi.org/10.2514/6.2017-2325>
 13. Hansmetzger, S., Zitoun, R., Vidal, P.: Detonation regimes in a small-scale RDE. In: 26rd International Colloquium on the Dynamics of Explosions and Reactive Systems, Boston, MA, USA (2017)
 14. Zhou, R., Wang, J.: Numerical investigation of shock wave reflections near the head ends of rotating detonation engines. *Shock Waves* **23**, 461–472 (2013). <https://doi.org/10.1007/s00193-013-0440-0>
 15. Yao, S., Han, X., Liu, Y., Wang, J.: Numerical study of rotating detonation engine with an array of injection holes. *Shock Waves* **27**, 467–476 (2017). <https://doi.org/10.1007/s00193-016-0692-6>
 16. Liu, S., Lin, Z., Liu, W., Lin, W., Zhuang, F.: Experimental realization of H₂/air continuous rotating detonation in a cylindrical combustor. *Combust. Sci. Technol.* **184**, 1302–1317 (2012). <https://doi.org/10.1080/00102202.2012.682669>
 17. Bykovskii, F.A., Zhdan, S.A., Vedernikov, E.F.: Continuous spin detonations. *J. Propuls. Power* **22**, 1204–1216 (2006). <https://doi.org/10.2514/1.17656>
 18. Liu, Y., Wang, J., Shi, T., Wang, Y., Li, Y., Li, Y.: Experimental investigation on the H₂/O₂ continuously rotating detonation engine. In: 24th International Colloquium on the Dynamics of Explosions and Reactive Systems, Paper 64, Taipei, Taiwan (2013)
 19. Wu, D., Zhou, R., Liu, M., Wang, J.: Numerical investigation of the stability of rotating detonation engines. *Combust. Sci. Technol.* **186**, 1699–1715 (2014). <https://doi.org/10.1080/00102202.2014.935641>
 20. Wang, Y., Wang, J.: Rotating detonation instabilities in hydrogen–oxygen mixture. *Appl. Mech. Mater.* **709**, 56–62 (2015). <https://doi.org/10.4028/www.scientific.net/AMM.709.56>
 21. Anand, V., St. George, A., Driscoll, R., Gutmark, E.: Statistical treatment of wave instability in rotating detonation combustors. 53rd AIAA Aerospace Sciences Meeting, Kissimmee, FL, USA, AIAA Paper 2015-1103 (2015). <https://doi.org/10.2514/6.2015-1103>
 22. Hishida, M., Fujiwara, T., Wolanski, P.: Fundamentals of rotating detonations. *Shock Waves* **19**, 1–10 (2009). <https://doi.org/10.1007/s00193-008-0178-2>
 23. Shimizu, H., Hayashi, A., Tsuboi, N.: Study of detailed chemical reaction model on hydrogen–air detonation. 39th AIAA Aerospace Sciences Meeting and Exhibit, Reno, NV, USA, AIAA Paper 2001-0478 (2001). <https://doi.org/10.2514/6.2001-478>
 24. Stull, D.R., Prophet, H.: JANAF Thermochemical Tables. The National Standard Reference Data System-National Bureau of Standards (NSRDS-NBS) 37, 2nd edn. Government Printing Office, Washington (1971)

Publisher's Note Springer Nature remains neutral with regard to jurisdictional claims in published maps and institutional affiliations.